International Journal of Nanomedicine

Dovepress
open access to scientific and medical research

Open Access Full Text Article

ORIGINAL RESEARCH

Fabrication of cRGD-modified reduction-sensitive nanocapsule via Pickering emulsion route to facilitate tumor-targeted delivery

This article was published in the following Dove Press journal:
International Journal of Nanomedicine

Xingxing Shang[1]
Qi Liu[2]
Tang Qin[1]
Xiaodi Xu[1]
Hongmei Sun[1]
Mingxing Liu[1]
Hongda Zhu[1]

[1]School of Food and Biological Engineering, National "111" Center for Cellular Regulation and Molecular Pharmaceutics, Key Laboratory of Fermentation Engineering (Ministry of Education), Hubei University of Technology, Wuhan, People's Republic of China; [2]Division of Pharmacoengineering and Molecular Pharmaceutics and Center for Nanotechnology in Drug Delivery, University of North Carolina at Chapel Hill, Chapel Hill, NC 27599, USA

Purpose: To fabricate multifunctional nanocapsule via Pickering emulsion route to facilitate tumor-targeted delivery.

Methods: Poly(N-isopropylacrylamide-co-acrylic acid) nanoparticles (PNA) stabilized nanocapsules were fabricated by Pickering emulsion (PE) technology. For controllable drug-release and enhancing targeted antitumor effects, the nanocapsules were crosslinked with cystamine and coupled on cell-surface molecule markers (cRGDfK) to achieve on-demand drug release and targeted delivery.

Results: The fabricated PE and nanocapsules with average particle sizes (250 and 150 nm) were obtained. Encapsulation efficiency of hydrophobic anticancer drug (DOX) was determined as >90%. Release kinetic profiles for encapsulated nanocapsules displayed circulation stability and redox-sensitive releasing behavior with the supposed increase bioavailability. Both cytotoxicity assay, cellular uptake analysis and anticancer efficacy in B16F10 murine model demonstrated these redox-responsive drug-release and active targeted delivery.

Conclusion: The results clearly demonstrated nanocapsule via PE route as promising candidate to provide an effective platform for incorporating hydrophobic drug for targeted cancer chemotherapy.

Keywords: nanocapsule, Pickering emulsion, control release, tumor-targeted delivery

Introduction

The use of nanocapsules has been considered an attractive and promising strategy for anticancer drug delivery since nanocapsules have the ability to effectively encapsulate therapeutic drugs, improve solubility, deliver the drug to targeted tissue or cells, and improve the therapeutic index of various chemotherapeutic.[1,2] Classical preparation methods, including emulsion–diffusion, nanoprecipitation, emulsion–coacervation, polymer-coating layer-by-layer were applied to prepare nanocapsules.[3,4] Among these various approaches, the emulsion–diffusion technique was one of the most prominent methods to prepare emulsion-based micro- or nano-capsules using small molecule surfactants,[5] proteins,[6] and colloidal particles as emulsifiers.[2,7] Recently, colloidal particles acting as particulate emulsifiers to fabricate nanocapsules based on Pickering emulsion (PE) technology have aroused great interest.[2,4,8–12] Compared to conventional emulsion technology, nanocapsules via PE route provide significant advantages in stabilization, tunable interfacial permeability, and enhanced controlled-release behavior.[7,13,14] Some researches

Correspondence: Hongda Zhu
School of Food and Biological Engineering, National "111" Center for Cellular Regulation and Molecular Pharmaceutics, Key Laboratory of Fermentation Engineering (Ministry of Education), Hubei University of Technology, Wuhan, Hubei Province 430068, People's Republic of China
Tel +861 327 704 4558
Email bszzhuhongda@yeah.net

submit your manuscript | www.dovepress.com
DovePress
http://doi.org/10.2147/IJN.S202063

suggested that soft nanoparticles due to their interfacial rheologic properties as emulsifiers had a more important influence on the stability of the system.[8,15] In our previous work, the deformable nanogels were used to fabricate nanoscale suprastructures via PE, which was capable of effective delivery of paclitaxel and prolonged blood circulation in vivo.[9] Nevertheless, the controlled release and targeted delivery of the payload remain a challenge for this delivery system.[1]

The nanocapsules with soft nanoparticle shells impart additional capabilities including controlled release of drug by responding to environmental stimuli (eg, pH or reduction).[14] So, a cross-linking strategy through a disulfide bond under tumor microenvironment stimuli has been utilized to solve stability and controlled-release problems.[16,17] Several groups reported that different structures of nanocarriers showed triggered drug-release behavior compared to their reduction-insensitive system and improved antitumor activity.[16,18,19] In addition, the utilization of special tumor cell-surface molecule markers can achieve cancer-targeted drug delivery. The $\alpha_v\beta_3$ integrin which is overexpressed in invasive tumors like melanomas, glioblastomas, breast, and colon was recognized by peptide analogs containing the RGD (Arg-Gly-Asp) sequence. So, RGD peptide analogs functionalized therapeutic system was a promising strategy for tumor-targeting treatment, such as micelles, liposome, and nanoparticles.[16,17,20]

Here, poly(N-isopropylacrylamide-co-acrylic acid) nanogel (PNA) stabilized nanocapsules were fabricated by PE technology. For enhancing antitumor effects and controllable drug release, the nanocapsules were crosslinked with cystamine to achieve circulation stability and reduction-sensitive drug release. A cyclic peptide c(Arg-Gly-Asp-d-Phe-Lys) (cRGD) was linked to the surface of reduction, crosslinking nanocapsules using EDC/NHS chemistry as the coupling technique (Scheme 1). cRGD coupling on redox-sensitive crosslinked nanocapsules via PE will be proposed as a nanocarrier for on-demand drug release and targeted delivery.

Material and methods

Materials

Acrylic acid (Sigma-Aldrich, China) was distilled before use. N,N'-methylenebisacrylamide and N-Isopropylacrylamide (J&K Scientific., Ltd., Shanghai, China) were recrystallized from methanol and n-hexane, respectively. Doxorubicin hydrochloride (DOX HCl) was purchased from Xianghe Shunda Fine Chemical Co., Ltd. (Wuhan, China). 1-Ethyl-3-(3-dimethylaminopropyl) carbodiimide hydrochloride (EDC.HCl), N-Hydroxysuccinimide (NHS), potassium persulfate, sodium dodecylsulfate, and 5-aminofluorescein were analytic grade and purchased from J&K Technology, Ltd. cRGD was synthesized by ABBiochem Co., Ltd. (Shanghai, China). DMEM and RPMI-1640medium were obtained from HyClone Laboratories, Inc. (Utah, USA). Trypsin was purchased from Gibco-BRL Life Technologies (Carlsbad, CA). Biosharp (Hefei, China) supplied DAPI and MTT. All other chemicals were analytical grade and used without further treatment.

Cell lines and murine tumor model

The mouse melanoma cell line B16F10 and human cervix adenocarcinoma cell line HeLa were obtained from

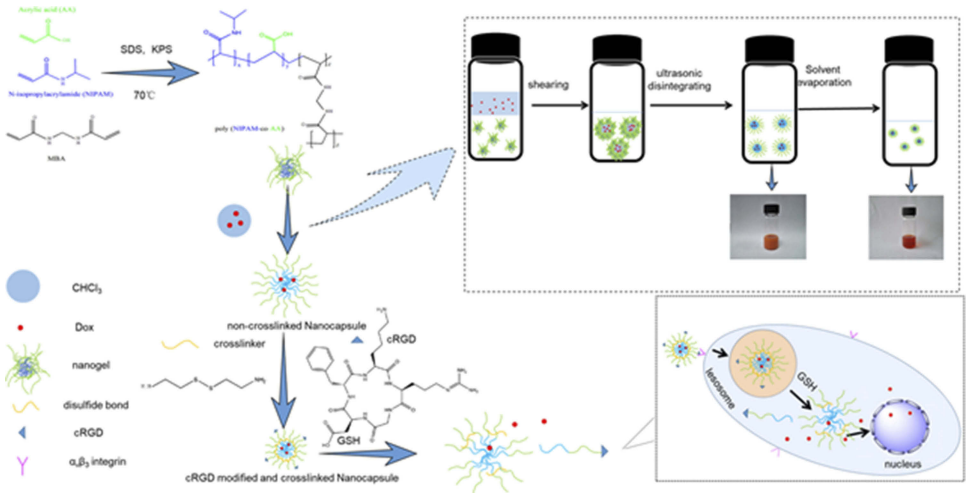

Scheme 1 Synthesis of PNA nanogels and fabrication of cRGD-modified reduction-sensitive nanocapsule via Pickering emulsion route for enhanced tumor targeted delivery.

CCTCC (Wuhan, China), which were cultured in DMEM and RPMI-1640 media containing 10% FBS, 10 IU/mL of penicillin and streptomycin at 37°C in a 5% CO_2 atmosphere.

C57BL/6 mice (female, 6–8 weeks) were purchased from the Laboratory Animal Center, Hubei Academy of Preventive Medicine (Wuhan, China). All animal studies were approved by the IACUC committees at Hubei University of technology, the care and use of animals were followed the guideline for welfare and ethics of laboratory animals in People's Republic of China. In this work, we used the murine B16F10 tumor model, which was subcutaneously inoculated with 1×10^6 B16F10 cells onto murine host. Once tumor volume grew to 200 mm^3 (length × width × width ×0.5), host was subject to therapeutic studies.

Preparation of PNA nanogel-stabilized PEs

PNA nanogels were synthesized using N-isopropylacrylamide and acrylic acid at a ratio of 10:1 with emulsion polymerization described before (Supporting information).[21] The aqueous phases of the nanogels (10 $mg\cdot mL^{-1}$) were obtained by dissolving freeze-dried PNA nanogels into water. The crude emulsion was prepared after shearing the mixture the aqueous phase and organic phase (Chloroform) at 13,000 rpm for 10 mins (Fluko FA25 homogenizer). The PEs were further obtained by ultra-sonicating the preliminary emulsion (400 W, 2:2, 4 mins) using an ultrasonic cell disruptor (JY92-IIN, Ningbo Scientz Biotechnology Co., Ltd., China) in an ice-water bath. The 5-aminofluorescein-labeled PNA nanogels (Supporting information) used to validate the location of nanogels in O/W emulsion surface. Using the same method, red fluorescent material (DOX) was encapsulated into the PEs.

Fabrication of cRGD-modified and redox-sensitive crosslinked nanocapsule (cRGD-ss-NCPE)

Nanocapsule via Pickering emulsion route (NCPE) was prepared using the PE solvent evaporation method to remove chloroform.[15] The redox-sensitive crosslinked nanocapsule was crosslinked by cystamine dihydrochloride using EDC/NHS chemistry coupling.[17] First, 5 mL of NCPE (pH=3.6–3.8) was activated by adding 3 mg of NHS and 10 mg of EDC. After the suspension was stirred for 30 mins, the pH value was adjusted to 6.8–7.2 with triethylamine. Then, cystamine dihydrochloride was added and reacted for 24 hrs at room temperature. The crosslinked cRGD-modified nanocapsule (cRGD-ss-NCPE) was prepared by mixing 1.69 mg cystamine dihydrochloride and 5 mg of cRGD peptide at the same time to the above-activated mixture for a further 24 hrs at room temperature. Finally, cRGD-ss-NCPE was dialyzed to remove redundant molecules. DOX was chosen as the model anticancer drug to assess the DOX-loaded NCPE (DOX-NCPE, or cRGD-DOX-ss-NCPE). For the encapsulation of DOX in nanocapsule via PE, DOX was dissolved in $CHCl_3$ to form the oily phase, and the PEs stabilized were prepared by 1% PNA nanogels. Then, DOX-loaded NCPE (0.5 $mg\cdot mL^{-1}$) was received according to the above method.

Characterization

Measurement of size distribution, zeta potential, and morphology

The average size, polydispersity index (PDI), and zeta potential of the NCPE and cRGD-ss-NCPE were observed by dynamic light scattering (DLS, Malvern Instrument, Malvern, UK). Morphology of nanogels and NCPE were determined through transmission electron microscopy (TEM, JEOL JEM-2100F, Japan). The PE with or without DOX, which were stabilized by 5-aminofluorescein-labeled PNA were observed by confocal microscopy (Perkin Elmer, UltraVIEW VoX, USA) for confirming the PE structure at the excitation (λex=490 nm) and emission (λem=525 nm) wavelengths.

Stability and reduction-triggered destabilization of NCPE

The physical stability of the NCPE and crosslinked-NCPE was inspected by DLS. The samples diluted with extensive dilution water (1:3,000) and the cell culture medium (DMEM, 1:100), and measured their sizes. The redox-sensitive evaluation of reduction crosslinked-NCPE was monitored in vitro by DLS. The sample solutions were diluted 10 fold with water and bubbled with N_2 for 15 mins, glutathione (GSH) was added to yield the final GSH concentration (10 mM) in a shaking bed at 37°C. The change of the sample's size was monitored at predetermined time intervals. The non-crosslinked NCPE acted as the control.

The crystal form determination of the DOX encapsulated in the NCPE

A differential scanning calorimeter (DSC, Perkin-Elmer Pyris Diamond) was used to observe the change in the crystal form of DOX with or without being encapsulated

by NCPE. Differential scanning calorimetry runs were performed over a temperature range from 25°C to 400°C at a heating rate of 10°C per minute. Free DOX and blank NCPE were selected as the controls.

Drug loading efficiency

To investigate the drug loading amount (DL) and the entrapment efficiency (EE) of DOX-loaded NCPE formulations, 1.0 mL DOX-NCPE or cRGD-DOX-ss-NCPE were added to ultrafiltration tube (Minipore, 10KMWCO, 4 mL) and then centrifuged (3,000 rpm for 1 hr). The resulting filtrate was performed by fluorospectrophotometry (F4500, Hitachi Co., Japan) with the measured condition (λ(ex)=498 nm, λ(em)=556 nm). EE (%) and DL (%) were calculated as follows:

$$EE\,(\%) = \left(W_0 - C_f.V_f\right)/W_0 \times 100\%$$

$$DL\,(\%) = \left(W_0 - C_f.V_f\right)/W_s \times 100\%$$

Here, W_0 is the feeding amount of DOX and W_S is the weight of the DOX-NCPE after lyophilization, C_f and V_f are the concentration and volume of free DOX, respectively.

In vitro drug-release behaviors

The drug release from DOX-loaded NCPE formulation in different situations was evaluated using the dialysis technique. The aqueous suspensions of 1.0 mL of DOX-ss-NCPE were placed within dialysis tubes (MWCO of 8,000–14,000), which were immersed into PBS (0.1 mol.L^{-1}, pH=7.4,) with or without GSH (10 mmol.L^{-1}) and continuously shaken at 37°C. The dialysate samples were removed at prescribed time intervals using fluorescence measurement (λex=480 nm, λem=570 nm). Similarly, the release of DOX from DOX-NCPE in PBS was also monitored as a control group.

In vitro cytotoxicity assay and cellular uptake

To explore the biocompatibility of the blank nanocapsule and the antitumor ability of DOX-loaded NCPE formulation in vitro, a MTT assay was performed using B16F10 cells and HeLa cells. The empty series NCPE (NCPE, crosslinked NCPE, cRGD-ss-NCPE) and cRGD solution were diluted to the designed series concentration for biocompatibility test. Then, DOX, DOX-NCPE, DOX-ss-NCPE, cRGD-DOX-ss-NCPE were diluted to the designed series concentration of DOX (from 0.01 to 10 μg.mL^{-1}) with culture medium. The cell viability was performed using the MTT assay after incubation for 24 hrs with a microplate reader (BioTek Epoch, USA). The concentration inhibited cell growth by 50% (IC_{50}) of formulations were calculated using GraphPad Prism software.

Cellular uptake and intracellular release behaviors of the DOX-loaded NCPE formulations were investigated by CLSM using B16F10 cells ($\alpha_v\beta_3$ integrin-positive cells) and HeLa cells ($\alpha_v\beta_3$ integrin negative cells). B16F10 cells and HeLa cells had been incubated with free DOX, DOX-ss-NCPE, and cRGD-DOX-ss-NCPE (concentration of DOX were 1 μg.mL^{-1}). Incubation was carried out at different time intervals (2 hrs, 6 hrs). Finally, the cells were fixed with 4% paraformaldehyde and cell nuclei were stained with DAPI. The images were made using CLSM.

In vivo anticancer efficacy and tumor permeability

The tumor-bearing mice (tumor volume about 180–200 mm^3) were divided into three groups randomly as follows (n=5–7 per group): (1) PBS group; (2) DOX solution group at 10 mg.kg^{-1}; (3) cRGD-DOX-ss-NCPE at 10 mg DOX/kg. For DOX solution group and cRGD-DOX-ss-NCPE group, Dox was administered *i.v.* from day 10 and injected every other day with 4 total administrations. Tumor size and weight were detected every other day. The antitumor efficiency was evaluated by comparing with the inhibition ratio (IR). IR (%)=$[(W_C - W_T)/W_C] \times 100$, here W_C and W_T, respectively represent the average tumor weights of PBS group and each therapeutic group. DOX as model drug and probe was loaded in nanocapsule for the imaging of nanocapsule distribution and permeability in tumor. DOX solution and cRGD-DOX-ss-NCPE were *i.v.* injected with a single dose of 10 mg DOX/kg on the tumor-bearing mice. Tumor tissues were collected 6-hr post-injection. To visualize DOX-loaded nanocapsule distribution and penetration, the tumor was lyophilized and sectioned. Images were taken by fluorescence microscopy (Nikon, Tokyo, Japan).

Statistical analysis

Data were shown as mean±SD and obtained from no less than three separate experiments. The significances of the differences were analyzed using a two-tailed Student's *t*-test and one-way ANOVA. *$p<0.05$; **$p<0.01$ and ***$p<0.001$ were considered statistically significant in all cases.

Results and discussion

Nanocapsule via PE route and characterization

A series of measurements were employed to verify the formations of the nanocapsule via PE from PNA nanogels. PNA nanogels displayed an average diameter of about 145.2 nm and a narrow size distribution (PDI<0.10) with negative zeta potentials. PE and NCPE stabilized by PNA nanogels were characterized using DLS. First, PNA, PE, NCPE, and cRGD-ss-NCPE had average diameter of about 143.2, 230.9, 153.4, and 151.9 nm, respectively (Figure 1), and uniform particle size distributions with PDI<0.20 (Table S1). The spherical poly(N-isopropylacrylamide) (PNIPAM)- based nanogels were found to have significant deformability of swelling-shrinkage in response to an external stimulus (eg, temperature) in our previous studies.[9,21,22] PNA nanogels have a highly deformable ability, where N-isopropylacrylamide was used as the scaffold of network-like nanogels with deformability.[23] TEM imaging of PNA (Figure 1C) also validated that PNA had a spherical loose morphology, which was similar to that of our previous nanogels.[9] TEM images of the PE droplets stabilized by PNA nanogels (Figure 1E) showed a capsule-like and inherently hollow morphology, which provided enough space for the drug entrapment, and the deformable PNA nanogels were arranged at O/W interface similar to cauliflower. The sizes of NCPE and cRGD-ss-NCPE decreased by about 100 nm due to remove the organic phase but little change in size and PDI were observed after crosslinking by cystamine or cRGD modification. Figure 1D and F showed that DOX-NCPE and cRGD-DOX-ss-NCPE displayed a core-shell structure, which had a compact hydrophobic core and a loose hydrophilic shell. Disulfide crosslinking provided an opportunity for triggered drug release due to the existence of abundant reducing substances such as glutathione in cancer cells, which has provided for reversible stabilization.[24] The zeta potential of PNA, PE, NCPE, and cRGD-ss-NCPE were −12.5, −22.5, −19.2, and −17.6 mV, respectively (Table S1). Zeta potential of nanostuctures were negative due to existence of free carboxyl groups on the surface. The negative charges of NCPE and cRGD-ss-NCPE could reduce clearance by the reticulo-endothelial system (RES) due to the low absorption of plasma proteins.[25]

To validate the distribution of the PNA during the formation process of PE, 5-aminofluorescein was conjugated to PNA nanogels via amide (Supporting information). Imaging showed that green color presented at the interfaces of the droplets, possibly ascribed to the 5-aminofluorescein-labeled PNA nanogels around emulsion droplets (Figure 2B). DOX (5 $\mu g.mL^{-1}$) as a fluorescent dye was also encapsulated into the PE. The red fluorescence was observed in the inner oily droplets and coexisted at the O/W surface (Figure 3C), and a yellow-green color from 5-aminofluorescein-labeled PNA nanogels surrounding PE droplets existed (Figure 2D). PE was an emulsion that was stabilized by solid, nano- or micro-particles in the

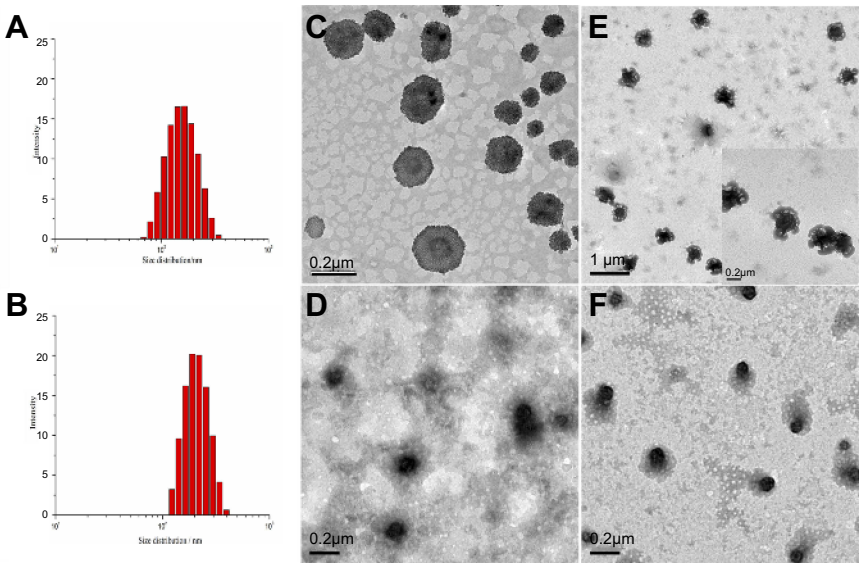

Figure 1 Particle size, size distributions and morphologies of PNA nanogels, Pickering nano-emulsions (PE), and nanocapsule formulations via Pickering emulsion route (NCPE). (**A**) Particle size of PNA nanogels (average diameter of 143.2 nm from DLS). (**B**) Particle size of PE (average diameter of 230.9 nm from DLS). (**C**) TEM images of PNA nanogels. (**D**) TEM images of DOX- NCPE. (**E**) TEM images of the Pickering emulsions stabilized by PNA nanogels. (**F**) TEM images cRGD-DOX-ss-NCPE.

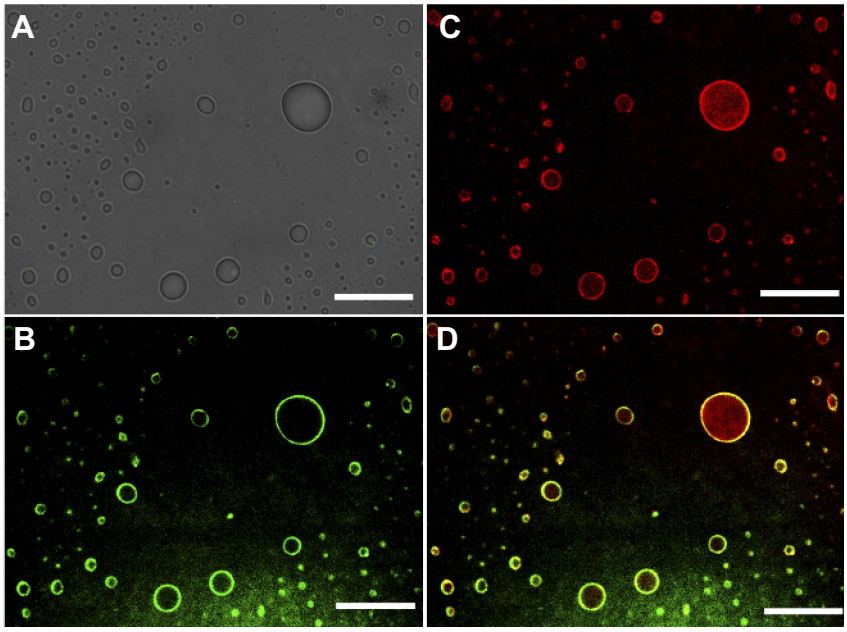

Figure 2 Fluorescent and optical images of the Pickering emulsions. (**A**) Optical image of the Pickering emulsion stabilized by 5-aminofluorescein labeled PNA nanogels. (**B** and **C**) Fluorescent images of the DOX-loaded Pickering emulsions stabilized by 5-aminofluorescein labeled PNA nanogels (5-aminofluorescein-labeled PNA nanogels show green fluorescent, DOX Show red fluorescent). (**D**) Fluorescent merged image of the Pickering emulsions containing DOX, stabilized by 5-aminofluorescein-labeled PNA nanogels. Scale bar = 5 μm.

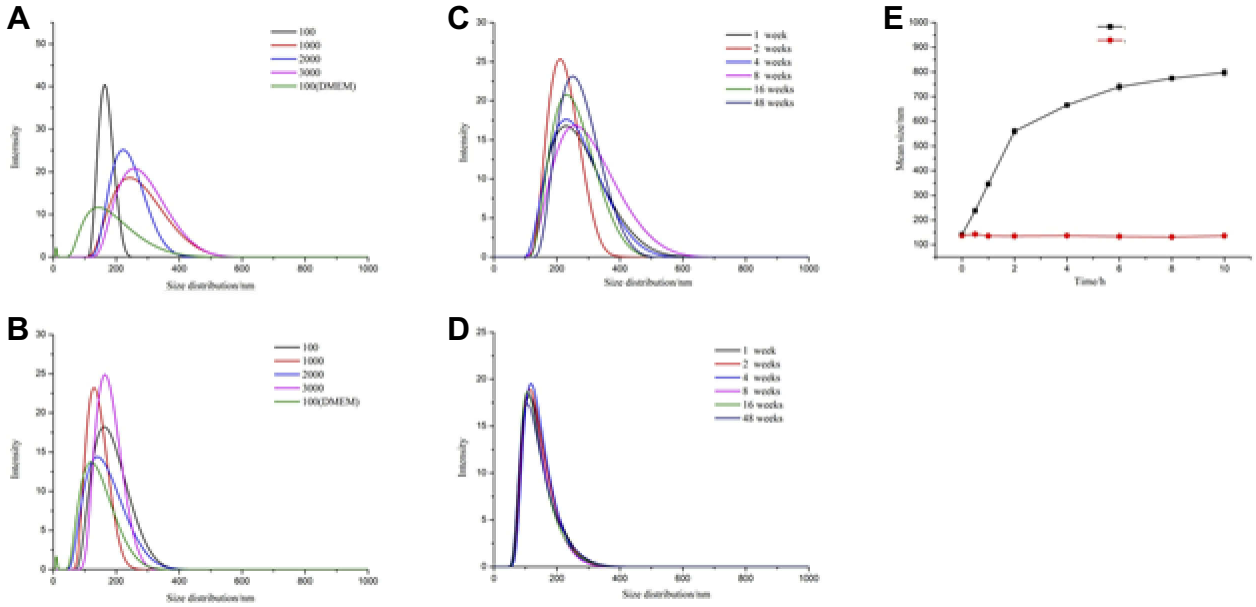

Figure 3 Comparison of stability of non-crosslinked NCPE (**A**) and cRGD-ss-NCPE (**B**) against dilution by water (3000 fold) and DMEM (100 fold). (**C** and **D**) the stability of non-crosslinked NCPE (**C**) and cRGD-ss-NCPE (**D**) during storage time respectively. (**E**) the redox-induced size variation of cRGD-ss-NCPE in the presence or absence of 10 mM GSH.

common sense.[8] Several groups and our previous work found that soft particles like PNIPAM-based nanogels could stabilize and fabricate PE.[9,15,26] Here, PNA where P-Nisopropylacrylamide was used as the scaffold of nanogels with deformability,[26,27] acrylic acid was copolymerized to improve hydrophilicity and provide an active site for crosslink or modification. Our result revealed that PNIPAM-based PNA nanogels had a highly deformable

ability, could arrange at O/W interfaces perfectly. Then, TEM imaging (Figure 1E) showed that the PE displayed capsule-like structures and matched with the fluorescent imaging (Figure 2) of the PE.

To improve circulation stability of the nanocapsule and prevent drug leakage in blood circulation, the nanocapsule was crosslinked by reversible disulfide bond.[28] Stability of NCPE and cRGD-ss-NCPE against extensive dilution and cell medium and storage time was investigated using DLS. In Figure 3, there were no significant changes in the average size of NCPE and cRGD-ss-NCPE for 48 weeks at room temperature, which demonstrated long-term stability of the NCPE formulations (Figure 3C). However, narrow and stable particle size distribution of cRGD-ss-NCPE compared to NCPE could be observed (Figure 3D). The results suggested that the disulfide bond crosslinking in NCPE could enhance the stability of this nanocarrier. As showed in Figure 3A, the size of the NCPE increased from 150 to 500 nm after 3,000 fold dilution with water and particle size distribution increased after 10-fold dilution with DMEM. The size and size distribution of nanocapsules increased due to naocapsules not enough stable and assembling large size nanocapsules under extensive dilution or similar humoral environments. In contrast, no size or size distribution changes were observed for cRGD-ss-NCPE under the same dilution conditions (Figure 3B). The results revealed that cRGD-ss-NCPE could retain the nanocapsule structure and improve circulation stability of the nanocapsule, which is highly favorable for bio-application.

The change of cRGD-ss-NCPE size in response to 10 mM GSH was monitored at various time intervals using DLS to prove the redox-stimulant cleavage of the disulfide bond in cRGD-ss-NCPE. In Figure 3E, the size change of cRGD-ss-NCPE was from 141.5 to 597 nm when in the media with 10 mM GSH. However, there were no significant changes in cRGD-ss-NCPE in the media without GSH for 10 hrs. These results indicated that crosslinking of the nanocapsule with the disulfide bond could de-crosslink under a reducing microenvironment, which could retain systemic circulation stability and control drug release in response to reducing stimuli.

The drug loading of nanocapsule via PE and in vitro releasing behavior

Nanogels based on PNIPAM have been used extensively for drug delivery, but it was limited to load hydrophilic drugs and poor control-releasing properties.[29] We found that paclitaxel as a hydrophobic anticancer drug could be well encapsulated into PE nano-droplets stabilized by deformable nanogels and showed excellent release profiles in our previous research.[9] Here, DOX as a hydrophobic anticancer drug model has demonstrated the loading capability of the nanocapsule via PE route as a drug carrier. The results showed that NCPE had high encapsulation efficiency (EE) of 98±1.7% (w/w) similar to the report and drug loading capacity of 4.2 ±0.2% (w/w) for DOX. After crosslinking disulfide bond and cRGD modification, the EE and the loading efficiency of cRGD-DOX-ss-NCPE had only slightly decreased to 97.1±1.9% and 4.0±0.19%. The O/W PE nano-droplets could provide larger hydrophobic space to load DOX at the beginning of the nanocapsule process, so nanocapsule showed high drug encapsulation capacity. After removing chloroform, a part of the hydrophobic DOX was encapsulated into the nanocapsule and some transferred into 3D networks of PNA nanogels,

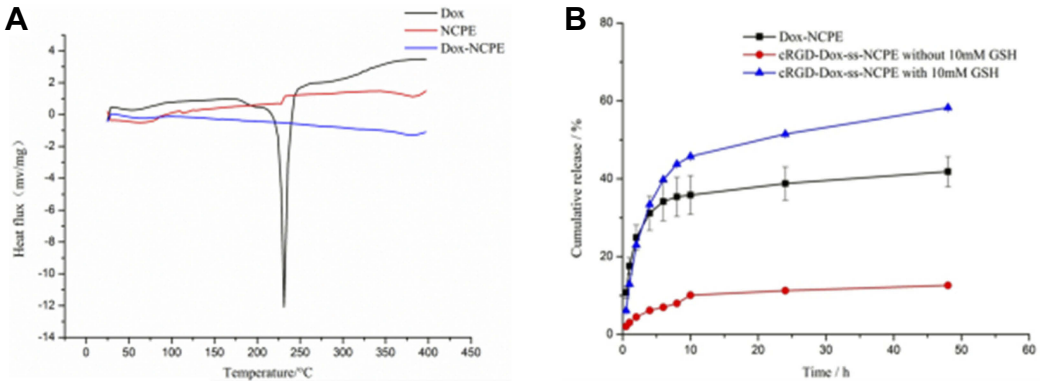

Figure 4 (**A**) DSC curves of Dox, NCPE and Dox-NCPE. (**B**) In vitro drug release of Dox-NCPE and cRGD-Dox-ss-NCPE with or without 10 mM GSH. Data are presented as mean ± SD (n=3).

which were validated using fluorescent imaging (Figure 2C and D).

Some studies revealed that poorly water-soluble drugs presented in amorphous conditions and lost crystallinity to improve drug solubility and bioavailability.[30] Here, differential scanning calorimetry (DSC) was used to observe the reduction in crystallinity peaks of DOX. Figure 4A depicts the DSC thermograms of pure DOX powder, NCPE, and DOX-loaded NCPE. DOX powder exhibited a single endothermic peak at 231°C. However, the sharp endothermic peak of DOX-loaded NCPE disappeared. Similar to blank NCPE, it was attributed to the existence of the DOX change from a crystalline to an amorphous form.

Favorable drug delivery systems include efficiency drug-loading capacity, controllable drug-release behavior and biodegradability profiles. Burst release or drug leakage in circulation due to nanocarrier instability would reduce therapeutic effects, which is a huge challenge for drug delivery system in vivo.[32] The stimuli-sensitive nanocarriers could respond to extra- and intracellular biological signal such as redox potential, pH, light, temperature.[33] The reduction responsive due to its superior extracellular stability and rapid intracellular drug release hold great potential.[34,35] The release of DOX from DOX-NCPE and DOX-ss-NCPE in vitro was monitored at 37°C in PBS (0.1 M, pH=7.4) with or without GSH (10 mM) to validate circulation stability and redox-sensitive intracellular delivery of nanocapsule. In the presence of GSH (Figure 4B), DOX-ss-NCPE released quickly with about 50.0% cumulative release within 10 hrs, then released slowly with nearly 60.0% cumulative release up to 48 hrs, which was similar to the release profiles of DOX-NCPE in PBS without 10 mM GSH. As a comparison, DOX-ss-NCPE in the absence of GSH only released with less than 10% cumulative release over a period of 10 hrs The remarkable decrease suggested that nanocapsule crosslinked with disulfide bond could prevent DOX leakage at a normal environment

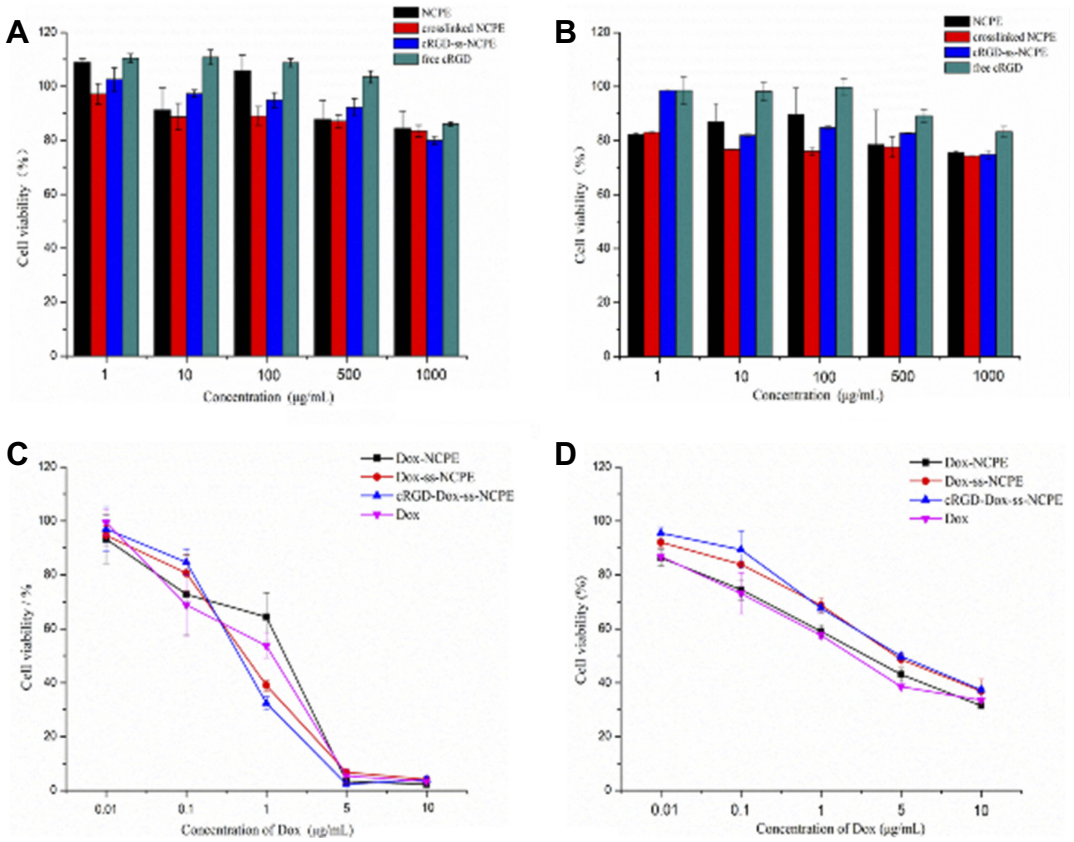

Figure 5 **A** and **B**, Cell cytotoxicity of blank NCPE (NCPE, crosslinked NCPE and cRGD-ss-NCPE) and free cRGD solution after 24 hours incubation using B16F10 cells (**A**) and HeLa cells (**C** and **D**) Cell cytotoxicity of Dox-loaded NCPE (Dox-NCPE, Dox-ss-NCPE and cRGD-Dox-ss-NCPE) and free Dox after 24 hours incubation using B16F10cells (**C**) and HeLa cells (**D**).

in vivo and trigger elective release under a reducing microenvironment.

In vitro cytotoxicity assay and cellular uptake

The biocompatibility of NCPE and the cytotoxicity of DOX-loaded NCPE formulation were performed using the MTT assay. In Figure 5A and B, blank NCPE, cRGD-ss-NCPE and cRGD did not exhibit significant cytotoxicity to B16F10 cells or HeLa cells (Cell Survival ≥80%) up to a tested concentration of 1,000 $\mu g \cdot mL^{-1}$, which indicated that NCPE as a nanocarrier has low toxicity and excellent biocompatibility.

As shown in Figure 5C and D, the cytotoxicity of DOX-loaded NCPE formulation at various DOX concentrations (0.01–10 $\mu g \cdot mL^{-1}$) was investigated using B16F10 cells and HeLa cells. Both DOX and DOX-loaded NCPE had a dose-dependent increased cytotoxicity. The viability of B16F10 cells incubated with DOX-cRGD-ss-NCPE exhibited a similar cytotoxicity with DOX, which revealed the NCPE formulations did not influence the cytotoxicity of DOX. Then, DOX-cRGD-ss-NCPE exhibited a high antitumor effect in $\alpha_v\beta_3$ overexpressing B16F10 cells with IC_{50} of 0.20 $\mu g \cdot mL^{-1}$, which was 1.5- and 1.6-fold lower than that of the DOX-NCPE (0.30 $\mu g \cdot mL^{-1}$) and DOX-ss-NCPE (0.32 $\mu g \cdot mL^{-1}$) control groups, respectively. Furthermore, the IC_{50} value of DOX-cRGD-ss-NCPE (2.2 $\mu g \cdot mL^{-1}$) in $\alpha_v\beta_3$ negative HeLa cell, which was 2.5- and 1.05-fold higher than the values of DOX (0.87 $\mu g \cdot mL^{-1}$) and DOX-ss-NCPE (2.1 $\mu g \cdot mL^{-1}$). The increased cytotoxicity of DOX-cRGD-ss-NCPE for $\alpha_v\beta_3$ overexpressing B16F10 cells owed to cRGD peptide-mediated cellular uptake. These results confirmed that active-targeting was critical for cRGD-ss-NCPE as a drug nanocarrier to achieve high antitumor activity.

CLSM was employed to research the cellular uptake behavior of various DOX-loaded NCPE formulation in $\alpha_v\beta_3$ integrin-positive cells (B16F10) and $\alpha_v\beta_3$ integrin-negative cells (HeLa). As showed in Figure 6A, DOX-ss-NCPE and DOX-cRGD-ss-NCPE showed significantly higher fluorescence than DOX; the DOX fluorescence intensity was enhanced when DOX was loaded into cRGD-ss-NCPE compared with DOX-ss-NCPE in B16F10 after incubations of 2 and 6 hrs (Figure 6B). However, the fluorescence of DOX was not significantly increased in $\alpha_v\beta_3$ integrin-negative HeLa cells (Figure 6C and D). cRGD-ss-NCPE as a drug carrier could enhance cRGD peptide-mediated cellular uptake and facilitate the release of DOX responding to intracellular reducing microenvironments. The above results indicated that cRGD-ss-NCPE as promising candidates to provide an effective platform for incorporating hydrophobic drug for targeted cancer chemotherapy.

In vivo anti-tumor efficacy

Here, DOX was chosen as the hydrophobic anticancer model to prove the potential of the nanocapsule to improve antitumor efficacy. DOX (10.0 $mg.kg^{-1}$) had significant tumor growth inhibition efficacy in the melanoma B16F10 subcutaneous model from day 10 to 22 in Figure 7A ($p<0.001$ compared with PBS group, n=5). Interestingly, cRGD-DOX-ss-NCPE group showed improved tumor growth inhibition efficacy than DOX HCL solution group from day 20 ($p<0.01$, n=5), and cRGD-DOX-ss-NCPE group achieved the highest antitumor efficacy among all groups. The result indicated the tumor-targeted nanocapsule could enhance the antitumor efficacy of DOX. The IRs based on the tumor weight (Figure 7B) were consistent with tumor volume measurement (Figure 7A).

DOX fluorescence intensity increased markedly in cRGD-DOX-ss-NCPE group compared with DOX HCL solution group (Figure 7D). The targeted and reduction-responded nanocapsules fabricated by PE should control drug releasing in suit and enhance the delivery of drug into the tumor. No significant loss of body weight (Figure 7C) demonstrated minor toxicity and low systemic toxicity for the treatment. It showed that nanocapsule displayed a potential for targeted cancer chemotherapy in nanomedicine.

Conclusion

In summary, the cRGD modified and reduction-sensitive nanocapsule was fabricated via PE route through assembling highly deformable and amphipathic PNA nanogels at O/W interfaces, which showed favorable stability, high EE, low cytotoxicity, and controlled release property. Fabricated nanocapsules with average particle size (150 nm) were obtained. EE of hydrophobic anticancer drug (DOX) was determined as >90%. Release kinetic profiles for encapsulated nanocapsules displayed circulation stability and redox-sensitive releasing behavior

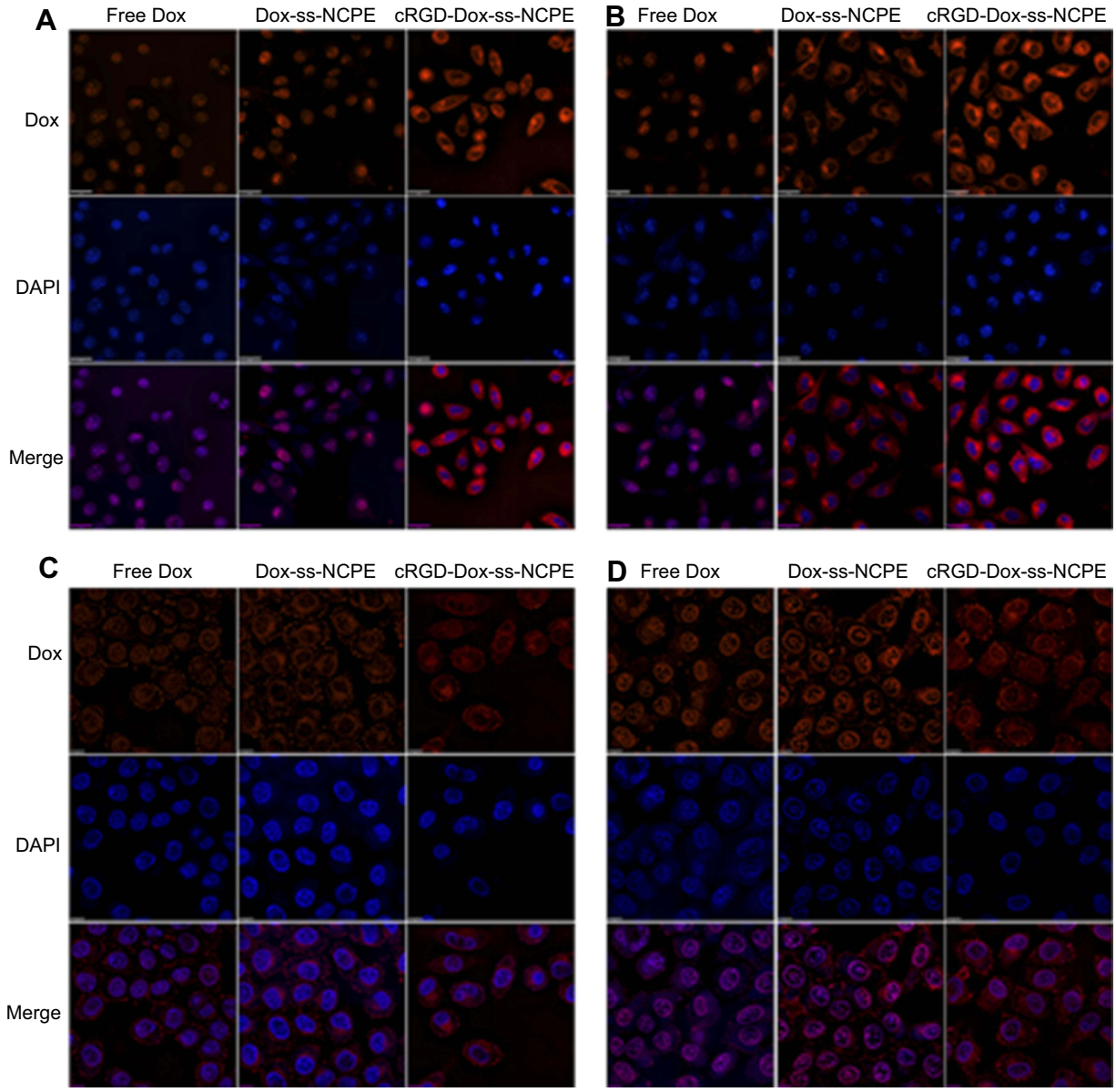

Figure 6 Cellular uptake of Free Dox, Dox-ss-NCPE and cRGD-Dox-ss-NCPE in B16F10 cells ($\alpha_v\beta_3$ intergrin-positive) (**A**, **B**) and HeLa cells ($\alpha_v\beta_3$ intergrin-negative) (**C**, **D**) visualized using CLSM, (**A** and **C**) 2 hours of incubation, (**B** and **D**) 6 hours of incubation. Nuclei were stained with DAPI. DAPI staining images and DOX images were merged. Scale bar = 20 μm.

without burst release when NCPE was crosslinked by reduction-cleavage of the disulfide bonds using cystamine dihydrochloride. Notably, cytotoxicity assay, cellular uptake analysis and anticancer efficacy in B16F10 murine model revealed efficiently target $\alpha_v\beta_3$ overexpressing tumor cell and control release in intracellular microenvironments. Therefore, cRGD-modified redox-sensitive nanocapsule via PE route as promising candidates provides an effective platform for incorporating hydrophobic drug for targeted cancer chemotherapy.

Acknowledgments

The authors would be supported by the National Natural Science Foundation of China (81201197 and 21501054), the Hubei Province Natural Science Fund Project (2015CFB588), and the Talents Program from Hubei University of Technology (BSQD12049).

Disclosure

The authors report no conflicts of interest in this work.

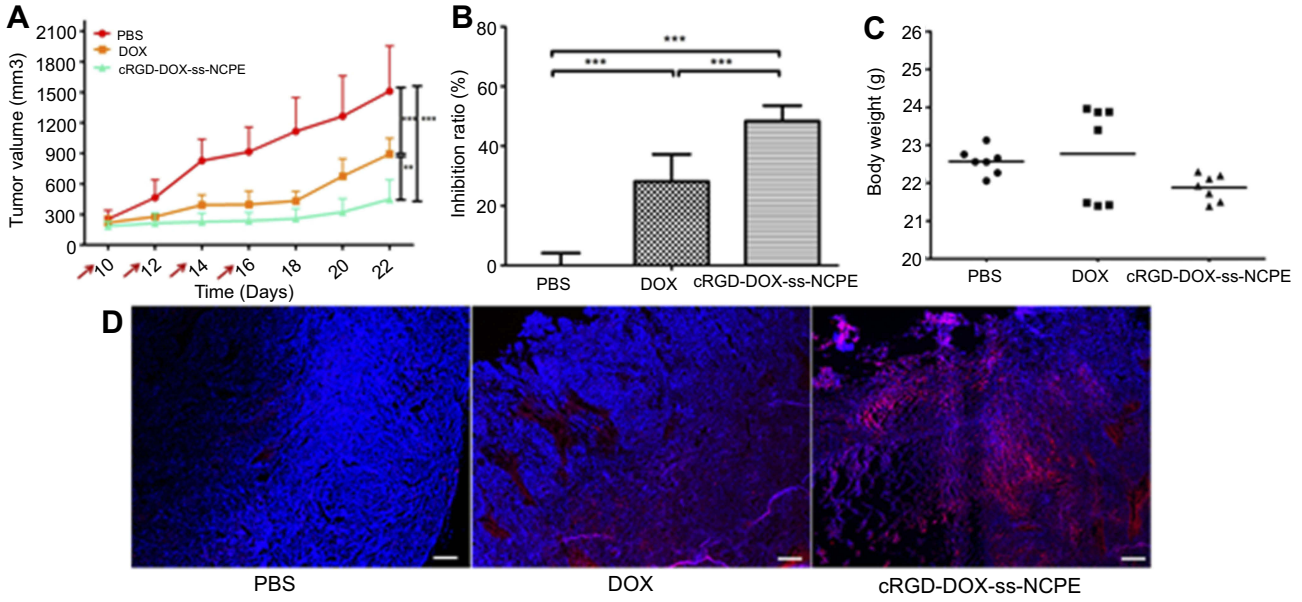

Figure 7 Anticancer efficacy in B16F10 murine model. Mice were subcutaneously inoculated on day 0 with 1×10^6 B16F10 cells. DOX and cRGD-DOX-ss-NCPE were administered *i.v.* from day 10 and injected every other day at a dose of 10 mg DOX/kg with 4 total administrations, respectively. Body weight and tumor size were detected every two days. (**A**) Tumor volumes of mice in each treatment group via time. The red arrows indicate the time of drug administration (n=5-7). (**B**) The body weight of treatment groups. (**C**) Tumor inhibition ratio. (**D**) Tumor permeability of DOX, DAPI (blue) stained the cell nuclei, and the white scale bar represents 100 μm. $^{**}p < 0.01$, $^{***}p < 0.001$.

References

1. Jeong Y, Kim ST, Jiang Y, et al. Nanoparticle-dendrimer hybrid nanocapsules for therapeutic delivery. *Nanomedicine-Uk*. 2016;11(12):1571–1578. doi:10.2217/nnm-2016-0034
2. Asabuwa Ngwabebhoh F, Ilkar Erdagi S, Yildiz U. Pickering emulsions stabilized nanocellulosic-based nanoparticles for coumarin and curcumin nanoencapsulations: in vitro release, anticancer and antimicrobial activities. *Carbohydr Polym*. 2018;201:317–328. doi:10.1016/j.carbpol.2018.08.079
3. Mora-Huertas CE, Fessi H, Elaissari A. Polymer-based nanocapsules for drug delivery. *Int J Pharm*. 2010;385(1–2):113–142. doi:10.1016/j.ijpharm.2009.10.018
4. Bollhorst T, Rezwan K, Maas M. Colloidal capsules: nano- and microcapsules with colloidal particle shells. *Chem Soc Rev*. 2017;46(8):2091–2126. doi:10.1039/c6cs00632a
5. Grigoriev DO, Bukreeva T, Mohwald H, Shchukin DG. New method for fabrication of loaded micro- and nanocontainers: emulsion encapsulation by polyelectrolyte layer-by-layer deposition on the liquid core. *Langmuir*. 2008;24(3):999–1004. doi:10.1021/la702873f
6. Rossier-Miranda FJ, Schroen K, Boom R. Microcapsule production by an hybrid colloidosome-layer-by-layer technique. *Food Hydrocolloid*. 2012;27(1):119–125. doi:10.1016/j.foodhyd.2011.08.007
7. Hu SH, Liao BJ, Chiang CS, Chen PJ, Chen IW, Chen SY. Core-shell nanocapsules stabilized by single-component polymer and nanoparticles for magneto-chemotherapy/hyperthermia with multiple drugs. *Adv Mater*. 2012;24(27):3627–3632. doi:10.1002/adma.201201251
8. Piao SH, Kwon SH, Zhang WL, Choi HJ. Celebrating Soft Matter's 10th anniversary: stimuli-responsive Pickering emulsion polymerized smart fluids. *Soft Matter*. 2015;11(4):646–654. doi:10.1039/c4sm02393e
9. Chen H, Zhu H, Hu J, et al. Highly compressed assembly of deformable nanogels into nanoscale suprastructures and their application in nanomedicine. *ACS Nano*. 2011;5(4):2671–2680. doi:10.1021/nn102888c
10. Yang XC, Samanta B, Agasti SS, et al. Drug delivery using nanoparticle-stabilized nanocapsules. *Angew Chem Int Edit*. 2011;50(2):477–481. doi:10.1002/anie.201005662
11. Ali M, Mccoy TM, McKinnon IR, Majumder M, Tabor RF. Synthesis and characterization of graphene oxide-polystyrene composite capsules with aqueous cargo via a water-oil-water multiple emulsion templating route. *Acs Appl Mater Inter*. 2017;9(21):18187–18198. doi:10.1021/acsami.7b02576
12. Hu Y, Yang Y, Ning Y, Wang CY, Tong Z. Facile preparation of artemisia argyi oil-loaded antibacterial microcapsules by hydroxyapatite-stabilized Pickering emulsion templating. *Colloid Surf B*. 2013;112:96–102. doi:10.1016/j.colsurfb.2013.08.002
13. Wu R, Pan J, Dai X, et al. A hierarchical rippled and crumpled PLA microstructure generated through double emulsion: the interesting roles of Pickering nanoparticles. *Chem Commun (Camb)*. 2015;51:16251–16254. doi:10.1039/C5CC06516J
14. Yeh YC, Tang R, Mout R, Jeong Y, Rotello VM. Fabrication of multiresponsive bioactive nanocapsules through orthogonal self-assembly. *Angew Chem*. 2014;53(20):5137–5141. doi:10.1002/anie.201400559
15. Zhou GF, Zhao YB, Hu JD, Shen L, Liu W, Yang XL. A new drug-loading technique with high efficaciency and sustained-releasing ability via the Pickering emulsion interfacial assembly of temperature/pH-sensitive nanogels. *React Funct Polym*. 2013;73(11):1537–1543. doi:10.1016/j.reactfunctpolym.2013.08.004
16. Zhu YQ, Zhang J, Meng FH, et al. cRGD-functionalized reduction-sensitive shell-sheddable biodegradable micelles mediate enhanced doxorubicin delivery to human glioma xenografts in vivo. *J Controlled Release*. 2016;233:29–38. doi:10.1016/j.jconrel.2016.05.014

17. Cai M, Ye MY, Shang XX, et al. cRGD-functionalized redox-sensitive micelles as potential doxorubicin delivery carriers for alpha-(v)&(3) integrin over expressing tumors. *RSC Adv*. 2015;5 (112):92292–92302. doi:10.1039/C5RA16137A
18. Zhao MX, Biswas A, Hu BL, et al. Redox-responsive nanocapsules for intracellular protein delivery. *Biomaterials*. 2011;32 (22):5223–5230. doi:10.1016/j.biomaterials.2011.03.060
19. Lin WH, Sun TT, Xie ZG, Gu JK, Jing XB. A dual-responsive nanocapsule via disulfide-induced self-assembly for therapeutic agent delivery. *Chem Sci*. 2016;7(3):1846–1852. doi:10.1039/c5sc03707g
20. Diou O, Fattal E, Delplace V, et al. RGD decoration of PEGylated polyester nanocapsules of perfluorooctyl bromide for tumor imaging: influence of pre or post-functionalization on capsule morphology. *Eur J Pharm Biopharm*. 2014;87(1):170–177. doi:10.1016/j.ejpb.2013.12.003
21. Xiong W, Gao XA, Zhao YB, Xu HB, Yang XL. The dual temperature/pH-sensitive multiphase behavior of poly (N-isopropylacrylamide-co-acrylic acid) microgels for potential application in in situ gelling system. *Colloid Surf B*. 2011;84 (1):103–110. doi:10.1016/j.colsurfb.2010.12.017
22. Jiang LY, Zhou Q, Mu KT, et al. pH/temperature sensitive magnetic nanogels conjugated with Cy5.5-labled lactoferrin for MR and fluorescence imaging of glioma in rats. *Biomaterials*. 2013;34 (30):7418–7428. doi:10.1016/j.biomaterials.2013.05.078
23. Yang H, Wang Q, Li Z, et al. Hydrophobicity-adaptive nanogels for programmed anticancer drug delivery. *Nano Lett*. 2018;18:7909–7918. doi:10.1021/acs.nanolett.8b03828
24. Kuppusamy P, Li H, Ilangovan G, et al. Noninvasive imaging of tumor redox status and its modification by tissue glutathione levels. *Cancer Res*. 2002;62(1):307–312.
25. Concheiro A, Alvarez-Lorenzo C. Chemically cross-linked and grafted cyclodextrin hydrogels: from nanostructures to drug-eluting medical devices. *Adv Drug Deliver Rev*. 2013;65(9):1188–1203. doi:10.1016/j.addr.2013.04.015
26. Chacko RT, Ventura J, Zhuang J, Thayumanavan S. Polymer nanogels: a versatile nanoscopic drug delivery platform. *Adv Drug Deliv Rev*. 2012;64(9):836–851. doi:10.1016/j.addr.2012.02.002
27. Park JS, Yang HN, Woo DG, Jeon SY, Park KH. Poly (N-isopropylacrylamide-co-acrylic acid) nanogels for tracing and delivering genes to human mesenchymal stem cells. *Biomaterials*. 2013;34(34):8819–8834. doi:10.1016/j.biomaterials.2013.07.082
28. Chuan XX, Song Q, Lin JL, et al. Novel free-paclitaxel-loaded redox-responsive nanoparticles based on a disulfide-linked Poly(ethylene glycol)-Drug conjugate for intracellular drug delivery: synthesis, characterization, and antitumor activity in vitro and in vivo. *Mol Pharmaceut*. 2014;11(10):3656–3670. doi:10.1021/mp500399j
29. Sivaram AJ, Rajitha P, Maya S, Jayakumar R, Sabitha M. Nanogels for delivery, imaging and therapy. *Wires Nanomed Nanobi*. 2015;7 (4):509–533. doi:10.1002/wnan.1328
30. Vasconcelos T, Sarmento B, Costa P. Solid dispersions as strategy to improve oral bioavailability of poor water soluble drugs. *Drug Discov Today*. 2007;12(23–24):1068–1075. doi:10.1016/j.drudis.2007.09.005
31. Fontana MC, Beckenkamp A, Buffon A, Beck RCR. Controlled release of raloxifene by nanoencapsulation: effect on in vitro antiproliferative activity of human breast cancer cells. *Int J Nanomed*. 2014;9:2979–2991. doi:10.2147/IJN.S62857
32. Li YP, Xiao K, Zhu W, Deng WB, Lam KS. Stimuli-responsive cross-linked micelles for on-demand drug delivery against cancers. *Adv Drug Deliv Rev*. 2014;66:58–73. doi:10.1016/j.addr.2013.09.008
33. Zhou Q, Zhang L, Yang TH, Wu H. Stimuli-responsive polymeric micelles for drug delivery and cancer therapy. *Int J Nanomed*. 2018;13:2921–2942. doi:10.2147/IJN.S158696
34. Zhao LL, Liu C, Qiao ZZ, Yao Y, Luo JB. Reduction responsive and surface charge switchable polyurethane micelles with acid cleavable crosslinks for intracellular drug delivery. *RSC Adv*. 2018;8 (32):17888–17897. doi:10.1039/C8RA01581C
35. Zhane JM, Fang XB, Li ZY, et al. Redox-sensitive micelles composed of disulfide-linked Pluronic-linoleic acid for enhanced anticancer efficiency of brusatol. *Int J Nanomed*. 2018;13:939–956. doi:10.2147/IJN.S130696

Supplementary materials

Supporting information

1. Synthesis and Characterization of Poly (N-isopropylacrylamide-co-acrylic acid) nanogel (PNA)

Synthesis of PNA nanogels. The synthesis was carried via a modified surfactant-free emulsion polymerization method according to the published procedures[1]. At first, 1.415 g (2.5 mmol) of NIPAM, 0.09 g (0.25 mmol) of allylamine (AA), 0.085 g (2.75×10^{-2} mmol) of N, N'-methylene-bis-acrylamide (MBA) and 79.3 mg (0.055 mmol) of SDS dissolved in 200 ml of ultrapure water in a 250 ml three-necked flask. Afterward, the solution was sealed and bubbled under nitrogen for 20 min to remove the dissolved oxygen in the condition of 70 ºC with magnetic stirring at 1000 rpm. Polymerization was initiated by the rapid addition of KPS (63.15 mg, 0.047 mmol) and the reaction was kept at 70 ºC for 5 h under nitrogen. The solution was cooled to room temperature under continuous stirring and was dialyzed (MWCO= 14,000) for 1 week to remove SDS and unreacted monomers. After dialysis, the nanogels were freeze-dried and stored in a desiccator at room temperature.

Characterization of PNA nanogels. The average size, polydispersity index (PDI) and zeta potential of the PNA was determined through dynamic light scattering (DLS, Malvern Instrument, Malvern, UK). The morphology was observed through transmission electron microscopy (TEM, JEOL JEM-2100F, Japan).

2. Synthesis of Fluoresceinamine-labeled PNA nanogels

Firstly, 10 ml of the nanogels reconstitution fluid (10 $mg.mL^{-1}$) was actived by 6 mg of NHS and 20 mg of EDC for 30 min. Before acylation reaction, the pH value was adjusted to 6.8-7.2 using Triethylamine (TEA) and then 1 mg of 5-aminofluorescein was added and stirred another 4 h.The resultant was further purified by dialysis (the cutoff molecular weight is 14,000 Da) lasting 1 day with ultrapure water in order to remove the residual small molecules. Because of the light decomposition property of 5-aminofluorescein, the whole reactions should be carried out lucifugally.

3. Characterization of PNA, NCPE and DOX-loaded NCPE formulations

The average size, polydispersity index (PDI) and zeta potential of the NCPE and cRGD-ss-NCPE were detected by dynamic light scattering (DLS, Malvern Instrument, Malvern, UK), the samples were diluted 100-folds by water. The results were showed in Table S1.

Table S1 Size and zeta potential of PNA, NCPE and DOX-loaded NCPE formulations determined by DLS

Sample	Size(nm)	PDI	Zeta(mV)
PNA	145.2±5.3	0.068±0.04	−12.5±1.6
PE	249.2±3.5	0.067±0.04	−22.5±0.6
NCPE	153.4±4.5	0.067±0.05	−19.2±0.7
cRGD-ss-NCPE	151.9±5.2	0.124±0.01	−17.6±0.7
DOX-NCPE	142.6±1.5	0.118±0.07	−20.3±1.9
cRGD-DOX-ss-NCPE	139.2±1.5	0.08±0.03	−18.6±2.8

1. Chen H, Zhu H, Hu J, et al. Highly compressed assembly of deformable nanogels into nanoscale suprastructures and their application in nanomedicine. *Acs Nano*.. 2011;5(4):2671–2680.